Ultra-sensitive elemental analyzer/isotope ratio mass spectrometer for stable nitrogen and carbon isotope analyses

Nanako O. Ogawa[1,*], Toshi Nagata[2, 3], Hiroshi Kitazato[1], and Naohiko Ohkouchi[1]

Abstract

We modified an automated, continuous-flow elemental analyzer/isotope ratio mass spectrometer (EA/IRMS) system to improve sensitivity for precise determination of stable carbon and nitrogen isotopic compositions of organic matter. By optimizing the chromatography, reducing blank concentrations, and increasing the sample amount introduced to the ion source for mass spectrometry, we have succeeded in increasing practical sensitivity about 160−340 times for nitrogen and 30 times for carbon isotopic analyses, without losing high-throughput ability or analytical precision. With this system, we obtained analytical error for $\delta^{15}N$ of $\pm 0.1−0.2$‰ (1σ) for sample sizes $>$ 270 ngN and ± 0.4‰ (1σ) for 125−270 ngN. The analytical error for $\delta^{13}C$ for sample sizes >700 ngC was $< \pm 0.20$‰ (1σ).

INTRODUCTION

Compound-specific isotope analysis (CSIA) has conventionally been used as a tool for understanding various natural processes, including biogeochemical cycles, food web structures in the ecosystem, and climate change (e.g., Summons and Powell 1986; Hayes et al. 1987; Macko et al. 1987; Ohkouchi et al. 2005; Chikaraishi et al. 2007). The importance and utility of carbon, nitrogen, and hydrogen isotopic signatures of individual organic compounds from natural materials have been greatly enhanced since high-throughput on-line systems using gas chromatography/combustion/isotope ratio mass spectrometer (GC/
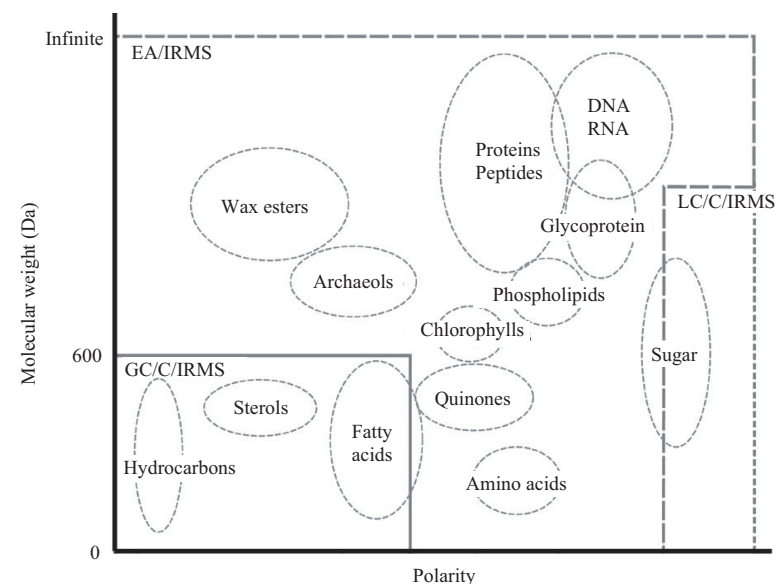
Fig. 1. Schematic distribution of various organic substances and the required equipment for their stable isotope analyses. The terms EA, GC/C, LC/C, and IRMS indicate elemental analyzer, gas chromatography/combustion, liquid chromatography/combustion, and isotope ratio mass spectrometer, respectively.

C/IRMS; Hayes et al. 1990; Brand 1996; Meier-Augenstein 1999) and elemental analyzer/ IRMS (EA/IRMS) became commercially available in the early 1990s. Recent development of the liquid chromatography/combustion/IRMS (LC/C/IRMS) system has further broadened the application of this technique, although the range of measurable organic compounds is still limited using this system (e.g., Caimi and Brenna 1993; Krummen et al. 2004; Tagami and Uchida 2008).

The EA/IRMS system provides isotopic compositions of both carbon and nitrogen in ~10 min per sample. However, the drawbacks of this system relative to GC/C/IRMS for the application of CSIA are two-fold: first, it requires isolation and purification of target compounds before isotopic analysis. Second and more seriously, the sensitivity of the conventional EA/IRMS system is much lower than that of the GC/C/IRMS system; EA/IRMS requires as much as 50 μgN and 20 μgC to precisely detect subtle changes in the isotopic compositions of natural materials. These quantities are more than 3 orders of magnitude larger than those required for GC/C/IRMS. Nevertheless, we believe that EA/IRMS is useful for CSIA, because it is able to determine the isotopic compositions of organic compounds with various polarities and molecular weights (Fig. 1). This is in contrast to GC/C/IRMS, whose practical analytical capacity is limited to relatively low polarity, low molecular weight (~600 Da) organic compounds.

In this study, to improve the sensitivity of the EA/IRMS system, we modified a conventional continuous-flow EA/IRMS system. This improvement expands the usefulness of CSIA in various areas, and thus contributes to further applications of CSIA as a technological basis for future research in isotope science.

Materials and methods

Standard organic compounds

We used analytical-grade tyrosine, alanine, and Ni-chelated octaethylporphyrin (Sigma-Aldrich Co.; Table 1). Their carbon and nitrogen isotopic compositions were carefully determined using conventional EA/IRMS by comparison with the analytical results of authentic international or laboratory standards. Tyrosine and alanine were finely pulverized and homogenized, whereas Ni-chelated octaethylporphyrin (Ni OEP) was dissolved in dioxin-analysis-grade ultra-pure chloroform (Wako Chemicals). Small amounts of powdered amino acid standards were weighed in pre-cleaned tin capsules and folded into tight pellets prior to placement on the autosampler of the EA/IRMS system. In contrast, an aliquot of the chloroform solution of Ni OEP was introduced into the tin capsule with a Pasteur pipette and slowly dried on a hot plate at 40−80°C. The sample capsule was carefully folded prior to isotope analysis.

Determination of carbon and nitrogen isotopic compositions

The isotope-ratio mass spectrometry system employed in this study was a ThermoFinnigan EA/IRMS system, an isotope ratio mass spectrometer (Delta plus XP IRMS) coupled to an elemental analyzer (Flash EA1112) interfaced *via* a continuous flow interface (ConFlo III). In this system, samples wrapped in tin capsules were combusted in the combustion (oxidation) column of the EA heated to 1050°C. The combustion products were then transferred by a carrier gas (He) to the reduction column with reduced copper at 750°C for reduction of nitrogen oxides to N_2 (Fig. 2). Water was removed as the effluent stream passed through the water trap column installed immediately after the reduction column, and the N_2 and CO_2 were separated on a gas chromatographic column (6 mm × 3 m, Porapak Q). The gas chromatographic effluents were then introduced into the continuous-flow interface, and delivered to a differentially pumped ion source for mass spectrometry through a capillary leak.

Carbon and nitrogen contents in the samples were determined using isotope ratio mass spectrometry with calibrated ion currents of *m/z* 44 and 28, respectively. The isotopic compositions were processed using ISODAT NT ver. 2.0 software and expressed in conventional δ notation:

$$\delta\ (\text{‰}) = (R_{sample}/R_{standard} - 1) \times 1000$$

where R represents the $^{13}C/^{12}C$ or $^{15}N/^{14}N$ ratio. Standards for carbon and nitrogen isotopes
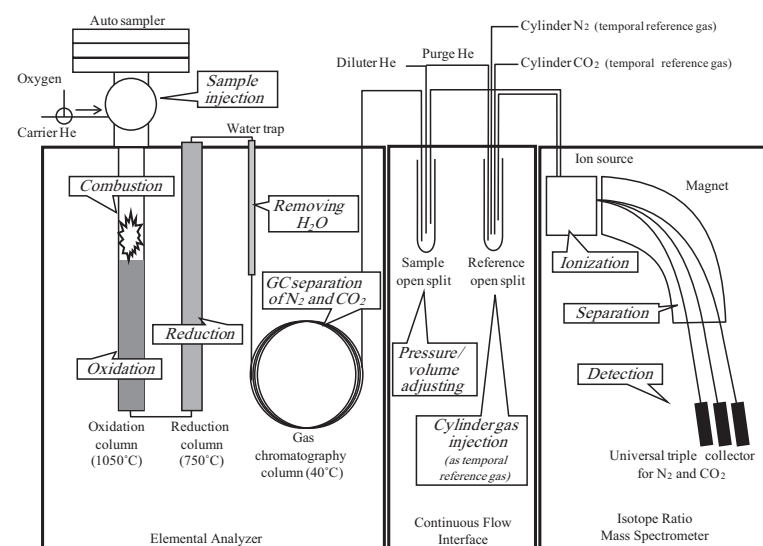
Fig. 2. Schematic image of the conventional EA/IRMS system. Samples are introduced to combustion, reduction, and water trap columns before separation into N_2 and CO_2 gases by gas chromatography. The continuous flow interface splits and reduces sample gas flow before introduction into the IRMS. Modifications were performed on the combustion/reduction columns, water trap, and oxygen/helium gas injection system of the EA and capillary tubes connecting the CF to the IRMS.

Table 1 List of organic chemicals used in this study.

Material	Source	M.W.	C/N (wt ratio)	TOC (wt% d.s.)	TN (wt% d.s.)
Alanine	Aldrich co.	89	2.6	40.5	15.8
Tyrosine	Aldrich co.	181	7.7	59.7	7.7
Ni-OEP	Aldrich co.	591	7.7	73.0	9.5

are Vienna Pee Dee Belemnite (VPDB) and atmospheric N_2 (AIR), respectively. All $\delta^{13}C$ and $\delta^{15}N$ values determined by the EA/IRMS and ISODAT NT software ($\delta^{13}C_{CF}$ and $\delta^{15}N_{CF}$) were corrected to account for instrumental drift by measuring laboratory standards interspersed among the samples. The $\delta^{13}C_{CF}$ and $\delta^{15}N_{CF}$ values of the laboratory standards were corrected to their known isotope values, and these corrections were applied to the $\delta^{13}C_{CF}$ and $\delta^{15}N_{CF}$ of the samples. Tyrosine, alanine, and Ni OEP (Table 1) were used as laboratory standards for this study. Analytical errors were estimated to be within 0.2‰ for both carbon and nitrogen based on repeated measurements of laboratory and authentic standards, unless otherwise noted.

Results and Discussion

Modification of the EA/IRMS system

There are three distinct approaches to improving the analytical sensitivity of the EA/IRMS system. They are 1) increasing the sample amount introduced to the ion source, 2) chromatographically improving the peak shapes of N_2 and CO_2, and 3) expanding the analytical range of IRMS by reducing interference from background contaminants. To these ends, we made several modifications to the conventional EA/IRMS system. First, the fused silica capillary column connecting the open-split in the ConFlo III interface and the ion source of the mass spectrometer was replaced with one with a larger inner diameter (0.15 mm i.d.) rather than a conventional capillary column with 0.10 mm i.d. This modification has the advantage that the amount of N_2 and CO_2 gases leaked to the ion source substantially increased. This modification, however, has the disadvantage of elevating pressure in the ion source, causing the load on the filament and the turbo molecular pumps to increase. Therefore, this modification potentially reduces their durability and working life. However, in our system, this disadvantage is generally offset by the accompanying benefit of reduced quantity of the introduced sample, which substantially reduces the load on the filament and turbo pumps.

Second, the quartz glass columns for the combustion and reduction furnaces and the water trap were replaced with narrow-diameter customized columns (Ogawa et al. patent pending). This modification substantially improved the peak shapes of N_2 and CO_2 gases on the chromatogram. The detected ion signals for N_2 (m/z 28) and CO_2 (m/z 44) of 0.13 mg tyrosine (equivalent to 10 μgN and 78 μgC) using the modified EA/IRMS system had peak shapes with height to width (H/W) ratios of 92 for N_2 and 226 for CO_2. These ratios are much better than those of the conventional system, for which the H/W ratios were 4.2 for N_2 and 9.2 for CO_2 (Fig. 3). It should be noted that the chromatographic peak shape is a critical factor in controlling the precision of the measured isotopic value, even when the amount of sample gas introduced to the ion source is constant.

For reduction of background contamination, we made two modifications. In the conventional EA/IRMS system, atmospheric nitrogen is generally a major source of contamination for nitrogen isotopic analysis, whereas impurities in the sample capsule are a source of background contamination for carbon isotopic analysis. To eliminate N_2 background contamination, we replaced the electric flow control valves of the EA used for pulse injection of oxygen into the commercial system with a leak-tight four-port valve (AR-UMF−4, GL Science Co.). This air-driven valve is automatically controlled by a custom-made electronic control module (Fig. 4). The outer housing of the valve was purged with analytical grade helium to prevent ambient air contamination through the rotary disc. The chamber-purging gas for the autosampler was also changed to oxygen from the default helium gas. The difference was significant, especially when extra sets of sample carousels were in use. For all of our analyses, the flow rate of the helium carrier and the oxygen gases
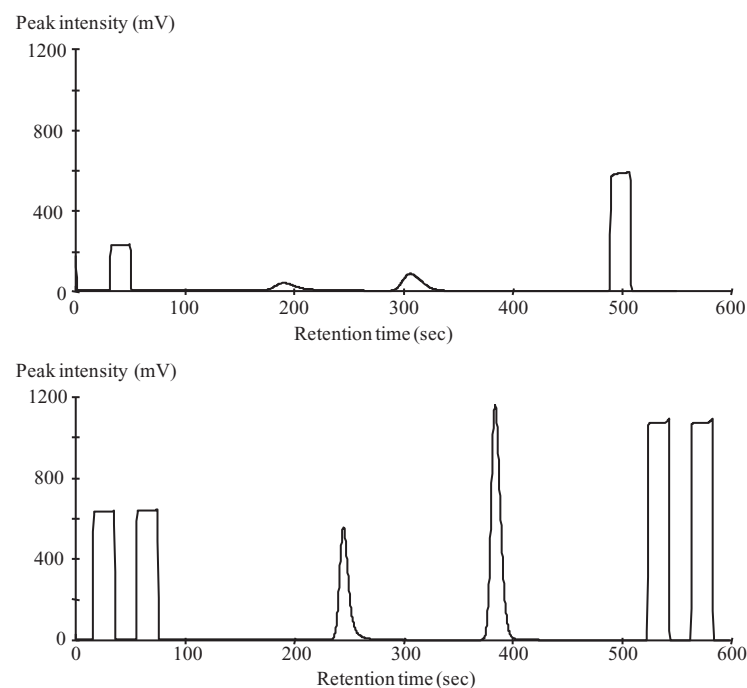
Peak intensity (mV)

Fig. 3. Detected signals for nitrogen (*m/z* 28) and carbon dioxide (*m/z* 44) measured by conventional (above) and modified (below) EA/IRMS. Introduced samples were 136 μg tyrosine for the conventional system and 133 μg tyrosine for the modified system. Square symbols in the earliest and the latest of the chromatogram are signals from the cylinder gases of N_2 and CO_2 being used as temporal isotope references for the analysis.

were set at 100 mL min^{-1}.

   The capsule blank is major source of background contamination for carbon. To investigate the magnitude of contamination in the capsule blank, various types of pre-cleaned sample capsules made of tin or silver were analyzed for carbon and nitrogen content using the EA/IRMS system. Little interference of nitrogen was detected in any of the capsules, whereas significant amounts of carbon were observed in all of the capsules (Table 2). Two commonly used types of thin foil capsules (5 mm o.d.), made of 99.9% and 97.5% tin, contained 0.86 ± 0.11 and 0.51 ± 0.07 μgC per capsule, respectively, even after washing with a mixture of organic solvents (methanol/dichloromethane, 1: 1, v/v) overnight. In contrast, a commercially supplied thick, hard tin capsule (2 or 4 mm o.d.) contained less carbon at 0.17−0.45 μgC per capsule, although they weighed more than the foil capsules (Table 2). Comparison between the different sizes (weights) of the hard capsules indicated that the larger (heavier) capsule contained more carbon. The silver foil capsule contained 0.64 ± 0.07 μgC per capsule, but combustion (400°C, 5 hours) reduced the blank level to 0.22
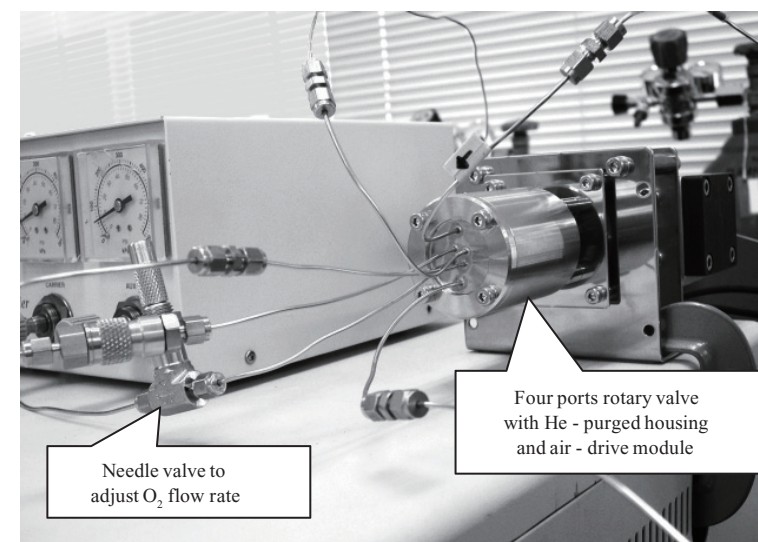

Fig. 4. Image of a four-port air-driven valve that was installed in the EA/IRMS system for reducing atmospheric contamination with nitrogen and carbon. A custom-made sequential controller unit was installed to link valve operation with the sequential analytical program of the IRMS.

Table 2 Carbon content in various pre-cleaned blank sample capsules.

Capsule type	Material	Size*	Weight (mg)	Preparation	C (ug/ capsule) ± sd	N (ug/ capsule) ± sd	n
Foil capsule	Sn 97.5%	5 × 9	33 ± 1	wash (MeOH/DCM)	0.51 ± 0.07	n.d.	(12)
	Sn 99.9%	5 × 9	33 ± 1	wash (MeOH/DCM)	0.86 ± 0.11	n.d.	(7)
	Ag 99.9%	5 × 9	37 ± 1	wash (MeOH/DCM)	0.64 ± 0.07	n.d.	(3)
	Ag 99.9%	5 × 9	37 ± 1	combustion (400°C 5hr.)	0.22 ± 0.02	n.d.	(3)
Hard container	Sn 99.9%	4 × 9	89 ± 1	wash (MeOH/DCM)	0.45 ± 0.07	n.d.	(3)
	Sn 99.9%	4 × 7	75 ± 1	wash (MeOH/DCM)	0.43 ± 0.03	n.d.	(3)
	Sn 99.9%	4 × 5.5	52 ± 1	wash (MeOH/DCM)	0.25 ± 0.05	n.d.	(27)
	Sn 99.9%	2 × 5		wash (MeOH/DCM)	0.17 ± 0.02	n.d.	(3)

* Capsule size was expressed as outer diameter (mm) × height (mm). Hard container was originally designed for liquid sample measurement and be sold as smooth surface capsule or smooth wall capsule.

± 0.02 μgC per capsule (Table 2).

Sensitivity, linearity, and blank correction

   The detected ion signals for N_2 (*m/z* 28) and CO_2 (*m/z* 44) were compared using the conventional and modified EA/IRMS systems (Figs. 5 and 6). With all of the modifications described above, the observed peak height per sample mass was multiplied by 13.5 for
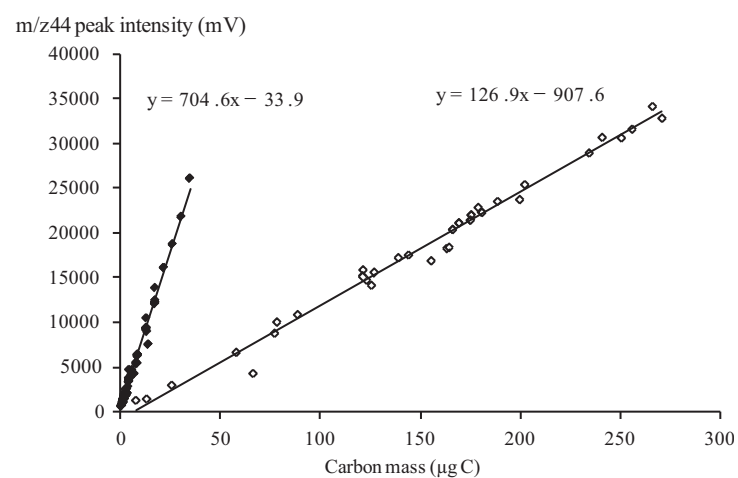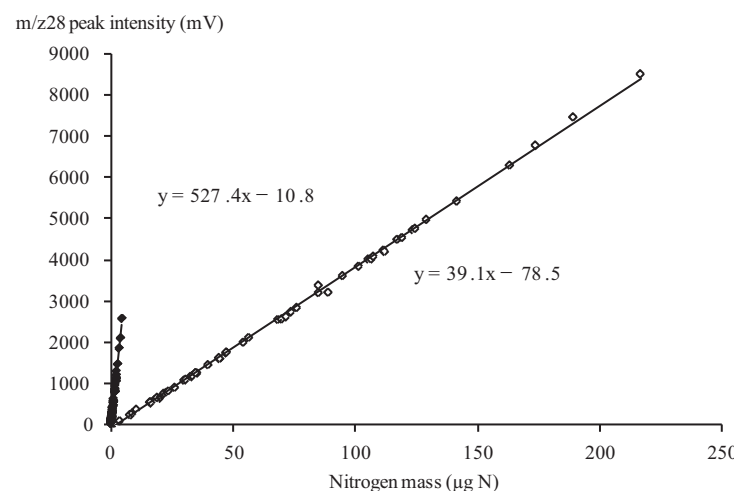
m/z28 peak intensity (mV)

$y = 527.4x - 10.8$

$y = 39.1x - 78.5$

Nitrogen mass (µg N)

m/z44 peak intensity (mV)

$y = 704.6x - 33.9$

$y = 126.9x - 907.6$

Carbon mass (µg C)

Fig. 5. Relationships between detected peak height (mV) and sample mass (µgN or µgC) obtained from conventional (open symbols) and modified (close symbols) EA/IRMS systems.

Nitrogen peak area (Vs)

$y = 0.81 x + 0.06$

$y = 3.87x - 0.05$

Nitrogen mass (µg N)

Carbon peak area (Vs)

$y = 14.3x - 1.8$

$y = 3.0x - 15.4$

Carbon mass (µg C)

Fig. 6. Relationships between detected peak areas and sample mass (µgN or µgC) obtained from conventional (open symbols) and modified (close symbols) EA/IRMS systems. Samples are the same as those depicted in Fig. 5.

N_2 and by 5.6 for CO_2, whereas the peak area, a more direct indicator of the amount of sample gas introduced into IRMS, was only multiplied by 4.8 for both N_2 and CO_2 relative to those of the commercial EA/IRMS system. These results strongly suggest that the gas chromatographic peak shape of the EA/IRMS system is a critical factor in reducing the required sample amount for isotopic analyses. The improvement in peak shape was more significant for nitrogen than for carbon.
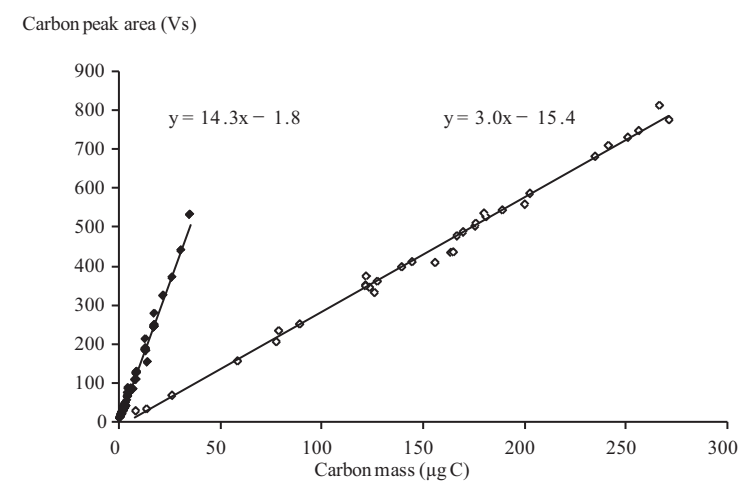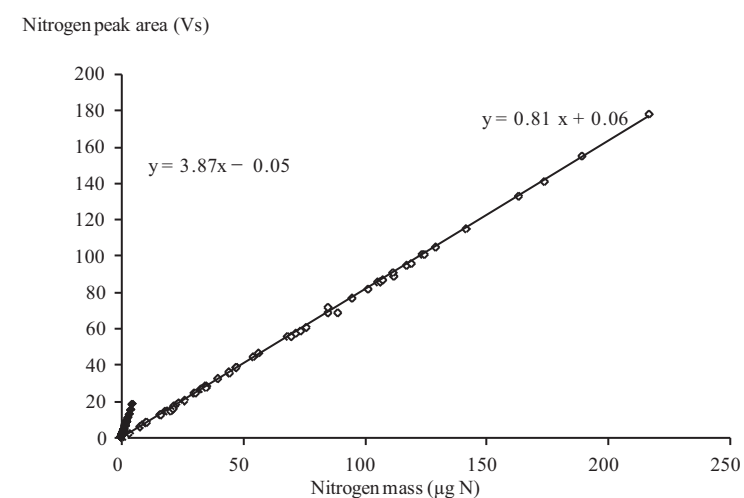
Figure 7 illustrates the differences between the measured and expected isotopic values ($\Delta\delta^{15}N$ and $\Delta\delta^{13}C$) for tyrosine, alanine, and Ni OEP with both the conventional and modified EA/IRMS systems. The observed $\Delta\delta^{15}N$ values for the conventional system exhibited significant drift for samples with <100 µgN, whereas the $\Delta\delta^{15}N$ for the modified EA/IRMS system showed no isotopic shift with sample size for samples >1 µgN. The apparent linearity of $\Delta\delta^{15}N$ extended to samples with as little as 90 ngN in the modified

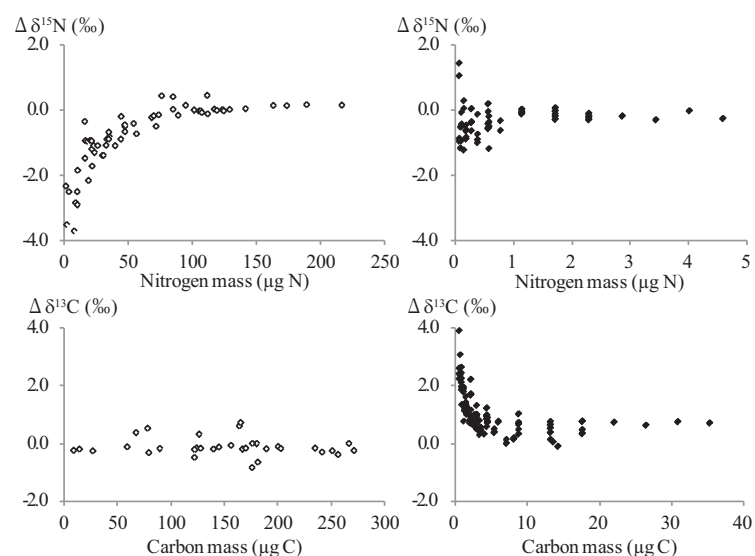**Fig. 7.** Distributions of Δδ¹⁵N and Δδ¹³C values obtained from conventional (open symbols) and modified (close symbols) EA/IRMS systems against sample mass. The values are expressed as differences from the correct and pre-calibrated values for each sample. Known isotope standards of tyrosine, alanine, and Ni-OEP (Table 1) were used as sample materials. Samples are the same as those depicted in Fig. 5.

system, although the smaller the sample size, the lower the precision. In other words, the minimum intensity of the ion peak for nitrogen (*m/z* 28 as N_2) to obtain ± 0.2‰ analytical error was improved from 2500 mV for the commercial system to 200 mV for the modified system. The minimum peak height corresponding to $< \pm 0.4$‰ error in the δ¹⁵N analysis was reduced to 100 mV. Accounting for increased intensity and practical analysis range (linearity), the sensitivity was 160−340 times greater for the modified system relative to the conventional system.

The linearity of Δδ¹³C, in contrast, extended only to 10 μgC for both the conventional and modified systems (Fig. 7). The difference arose due to contamination with carbon at detectable levels in both systems (Table 2). To improve the linearity of the carbon isotope analysis, blank correction was performed for every δ¹³C$_{CF}$ value, including the standards and the samples, using a simple mass balance equation as follows:

$$\delta^{13}C_{sample} = (\delta^{13}C_{measured} \cdot [Area]_{measured} - \delta^{13}C_{blank} \cdot [Area]_{blank}) / ([Area]_{measured} - [Area]_{blank})$$

where [Area] indicates the total *m/z* 44−46 peak area (Vs) calculated by the ISODAT NT software. The subscript "blank" represents the blank capsule. When the *m/z* 44 intensity of the blank capsule is smaller than the reliable analytical range of the IRMS (<100 mV), several blank capsules must be measured as a single sample to obtain a better δ¹³C$_{blank}$

Table 3 Analytical results for carbon and nitrogen isotope ratios by modified EA/IRMS

Range min ~ max	δ¹³C precision ± sd (‰, 1σ)	(n)	Range min ~ max	δ¹⁵N precision (sd ‰, 1σ)	(n)
Standard materials					
Ni-OEP					
970 ng C ~ 2.0 μg C	± 0.14‰	(7)	125 ng N ~ 270 ng N	± 0.40‰	(6)
2.2 μg C ~ 38.1 μg C	± 0.20‰	(23)	270 ng N ~ 4.8 μg N	± 0.19‰	(23)
Alanine					
0.7 μg C ~ 9.7 μg C	± 0.20‰	(8)	280 ng N ~ 3.8 μg N	± 0.12‰	(8)
Tyrosine					
4.6 μg C ~ 46.5 μg C	± 0.20‰	(13)	1.0 μg N ~ 6.0 μg N	± 0.17‰	(11)
Natural samples					
Chl. a (coral tree leaf)					
3.9 μg C ~ 5.8 μg C	± 0.02‰	(3)	333 ng N ~ 496 ng N	± 0.21‰	(3)
V-DPEP (Miocene rock)					
7.5 μg C ~ 9.1 μg C	± 0.10‰	(4)	700 ng N ~ 1390 ng N	± 0.20‰	(3)

value. Although this blank correction could be automatically performed by the ISODAT NT software, we do not recommend to apply this option because it is likely that an automatically applied δ¹³C$_{blank}$ value will not be accurate enough. After applying blank correction, the linearity of the Δδ¹³C reached 400 mV (equal to 700 ngC with a hard tin capsule).

Precision and limitations

Through the combined effect of these two improvements, the minimum sample amount required for high precision (± 0.2‰, 1σ) analysis was reduced to 270 ngN and 700 ngC (Table 3) for the modified EA/IRMS system. The minimum sample amount could be reduced to 125 ng for nitrogen if an analytical error of ± 0.4‰ (1σ) is acceptable, a somewhat poor number for conventional EA/IRMS but comparable to that of general GC/C/IRMS analysis (Chikaraishi and Oba 2008). Analytical error of the nitrogen isotope analysis for the amino acid standards ranging from 280 ng to 6.0 μg of nitrogen was 0.12‰ (1σ, n = 8, alanine) and 0.17‰ (1σ, n = 9, tyrosine). There are no data for the amino acid standards <10 μg bulk weight, due to the difficulty of weighing out extremely small amounts of powdered sample. The analytical error for the δ¹⁵N values of Ni OEP was ± 0.40‰ (1σ, n = 6) for 125−270 ngN. For samples with >270 ngN, the analytical error was substantially reduced to 0.19‰ (1σ, n = 23). The slightly poorer precision for the δ¹⁵N of Ni OEP relative to the amino acids is likely due to the lower combustion efficiency of the tetrapyrrole structure of Ni OEP.

The measured carbon isotopic compositions exhibited standard deviations of ± 0.20‰ for alanine, tyrosine, and Ni-OEP with carbon amounts >700 ngC. As discussed above, high background carbon interference has been a hindrance to low-level analysis, as the contaminant carbon mass in the sample capsules varied widely along with the size of the capsule itself.

Analytical precision was also tested for natural organic compounds (chlorophyll *a* and

alkyl porphyrin) extracted from natural samples and purified by HPLC (Chikaraishi et al. 2005; Kashiyama et al. 2007). The 1σ standard deviation for three separate analyses of these compounds ranged from ±0.02‰ to ±0.21‰ for $\delta^{15}N$ and $\delta^{13}C$ (Table 3). These results are considered to be comparable to CSIA (Chikaraishi and Oba 2008).

Applications of highly sensitive EA/IRMS

With the benefit of this highly sensitive EA/IRMS system, we have successfully expanded the potential applications of carbon and nitrogen isotopic studies. For example, detailed species-dependent biogeochemical processes of photoautotrophs in the natural environment were reconstructed using carbon and nitrogen isotopic signatures of small amounts of individual photosynthetic pigments (i.e., chlorophylls and bacteriochlorophylls) isolated and purified from meromictic lake water and sediments (Fig. 8a; Nakajima et al. 2004; Ohkouchi et al. 2005, 2008). Compound-specific isotope information for chlorophylls, bacteriochlorophylls, and isoprenoids enabled us to see difference in photosynthetic activities and substrate uptake processes between bacterial species and their surrounding aquatic environments. The isotopic analyses of alkyl porphyrins isolated from Cretaceous and Miocene organic-rich black shales provided information on the relative importance of N_2-fixing cyanobacteria as primary producers during the formation of these sediments (Fig. 8b; Ohkouchi et al. 2006; Kashiyama et al. 2007, 2008). The CSIA results suggested that diazotrophic cyanobacteria were the dominant components of primary production and N_2-fixation was a major process in the nitrogen assimilation, while the $\delta^{13}C_{porphyrin}$ suggested the dominance of β-carboxylation and/or active transport of carbon substrates, commonly conducted by cyanobacteria. For bulk isotope studies, the food web structure of the ecosystem at the deep sea floor was also successfully investigated using both carbon and nitrogen isotopic compositions of various benthic organisms, including benthic foraminifera (Fig. 8c; Nomaki et al. 2008). Bulk organic carbon and nitrogen isotope ratios were measured separately for each foraminifera species to access micro-food web structures and their importance to deep-sea environments. These applications could not have been achieved without development of the ultra-sensitive EA/IRMS system described in this chapter. These studies demonstrate that the reduction in sample requirement for both carbon and nitrogen isotope analyses by the EA/IRMS system greatly expands opportunities for environmental, ecological, and geological studies.

Conclusions

The overall result of these instrumental modifications reduced the amount of required sample size by two orders of magnitude compared to commercial EA/IRMS systems. At present, the minimum amounts of nitrogen and carbon required for precise (< ±0.2‰ analytical error) determination of isotopic compositions are 270 ngN and 700 ngC. With this system, 125 ng of nitrogen is required to achieve ±0.40‰ (1σ) analytical error.
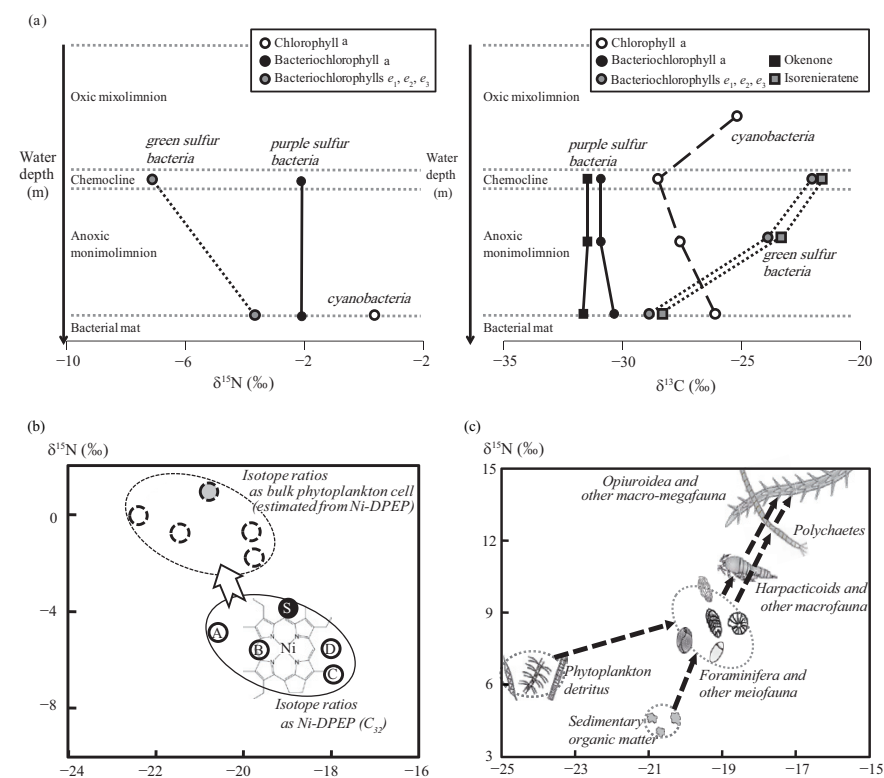
Fig. 8. (a) Distributions of nitrogen and carbon isotopic compositions ($\delta^{15}N$ and $\delta^{13}C$) of chloropigments and carotenoids isolated from Lake Kaiike (modified from Ohkouchi et al. 2005). (b) Distribution of $\delta^{15}N$ and $\delta^{13}C$ values of Ni-DPEP isolated from Cretaceous sedimentary rock (modified from Kashiyama et al. 2008). $\delta^{15}N$ and $\delta^{13}C$ of bulk phytoplankton cells were estimated by applying stable isotope ratio equations between tetrapyrrole nuclei and bulk organic cells of phytoplankton (Ohkouchi et al. 2006, 2007). (c) Schematic illustration of food web structures on the deep-sea floor (modified from Nomaki et al. 2008). Samples were collected from surface sediments of Sagami Bay, Japan at a water depth of 1430 m.

Improvements in the gas chromatographic peak shape and the sample/carrier dilution ratio both at the EA and ConFlo interface, which increase the intensity of the nitrogen and carbon ion peaks at the IRMS, were achieved by simple modifications of the columns and tube size. Reduction in air contamination to gain stability of the ion background in the IRMS, more effective for nitrogen than carbon, was achieved by introducing a custom-made leak-tight valve system for the EA. Reduction in the carbon background contamination was more difficult than for nitrogen, because the sample capsule was the primary source of contamination. The accuracy of the carbon isotope analysis, however, was improved by pre-cleaning the sample capsules and through mass-balance correction to omit the isotopic signal

of the capsules from that of the samples. Although the GC/C/IRMS is a mainstream CSIA technique, it is also true that the isotopic compositions of many biochemically important compounds cannot be determined by the system. To study these molecules, sophisticated preparative techniques, including high-performance liquid chromatography (e.g., Ohkouchi et al. 2005; Kashiyama et al. 2007) and preparative capillary gas chromatography (Eglinton et al. 1996) are required as well as the ultra-sensitive EA/IRMS described in this study.

Acknowledgments

The authors would like to thank Y. Chikaraishi and Y. Kashiyama for supporting laboratory work. This study was financially supported by JSPS, CREST-JST, and Grant-in-aid for Creative Scientific Research (19GS0211).

References

Brand WA (1996) High precision isotope ratio monitoring techniques in mass spectrometry. J Mass Spectrom 31: 225−235

Caimi RJ, Brenna JT (1993) High-precision liquid chromatography-combustion isotope ratio mass spectrometry. Anal Chem 65: 3497−3500

Chikaraishi Y, Matsumoto K, Kitazato H, Ohkouchi N (2007) Sources and transformation processes of pheopigments: stable carbon and hydrogen isotopic evidence from Lake Haruna, Japan. Org Geochem 38: 985−1001

Chikaraishi Y, Matsumoto K, Ogawa NO, Suga H, Kitazato H, Ohkouchi N (2005) Hydrogen, carbon, and nitrogen isotopic fractionations during chlorophyll biosynthesis in C3 higher plants. Phytochemistry 66: 911−920

Chikaraishi Y, Oba Y (2008) Compound-specific isotope analysis (CSIA) by gas chromatographic/isotope ratio mass spectrometer (GC/IRMS). Res Org Geochem 23/24: 99−122 (in Japanese)

Eglinton TI, Aluwihare LI, Bauer JE, Druffel ERM, McNichol AP (1996) Gas chromatographic isolation of individual compounds from complex matrices for radiocarbon dating. Anal Chem 68: 904−912

Hayes JM, Freeman KH, Popp BN, Hoham C (1990) Compound-specific isotopic analysis: a novel tool for the reconstruction of ancient biogeochemical processes. In: Durand B, Behar F (eds) Advances in Organic Geochemistry 1989, Pergamon Press, Oxford, pp. 1115−1128

Hayes JM, Takagiku R, Ocampo R, Callot HJ, Albrecht R (1987) Isotopic compositions and probable origins of organic molecules in the Eocene Messel shale. Nature 329: 48−51

Kashiyama Y, Kitazato H, Ohkouchi N (2007) An improved method for isolation and purification of sedimentary porphyrins by high-performance liquid chromatography for compound-specific isotope analysis. J Chromatogr A 1138: 73−83

Kashiyama Y, Ogawa NO, Kuroda J, Shiro M, Nomoto S, Tada R, Kitazato H, Ohkouchi N (2008) Diazotrophic cyanobacteria as the major photoautotrophs during mid-Cretaceous oceanic anoxic events: nitrogen and carbon isotopic evidence from sedimentary porphyrin. Org Geochem 39: 532−549

Krummen M, Hilkert AW, Juchelka D, Duhr A, Schluter H-J, Pesch R (2004) A new concept for isotope ratio monitoring liquid chromatography/mass spectrometry. Rapid Commun Mass Spectrom 18: 2260−2266

Macko SA, Fogel ML, Hare PE, Hoering TC (1987) Isotopic fractionation of stable nitrogen and carbon in

the synthesis of amino acids by microorganisms. Chem Geol (Isotope Geosci Sec) 65: 79−92

Meier-Augenstein W (1999) Applied gas chromatography coupled to isotope ratio mass spectrometry. J Chromatogr A 842: 351−371

Nakajima Y, Shimizu H, Ogawa NO, Sakamoto T, Okada H, Koba K, Kitazato H, Ohkouchi N (2004) Characterization of phototrophic sulfur bacteria in a saline meromictic Lake Abashiri based on chlorpigment stable isotopic compositions. Limnology 5: 185−189

Nomaki H, Ogawa NO, Ohkouchi N, Suga H, Toyofuku T, Shimanaga M, Nakatsuka T, Kitazato H (2008) Benthic foraminifera as trophic links between phytodetritus and benthic metazoans: carbon and nitrogen isotopic evidence. Mar Ecol Prog Ser 357: 153−164

Ohkouchi N, Kashiyama Y, Kuroda J, Ogawa NO, Kitazato H (2006) The importance of diazotrophic cyanobacteria as primary producers during Cretaceous Oceanic Anoxic Event 2. Biogeosciences 3: 467−478

Ohkouchi N, Nakajima Y, Ogawa NO, Suga H, Sakai S, Kitazato H (2008) Carbon isotopic composition of tetrapyrrole nucleus in chloropigments from a saline meromictic lake: a mechanistic view for interpreting isotopic signature of alkyl porphyrins in geological samples. Org Geochem 39: 521−531

Ohkouchi N, Nakajima Y, Okada, H, Ogawa NO, Suga H, Oguri K, Kitazato H (2005) Biogeochemical processes in a meromictic Lake Kaiike: implications from carbon and nitrogen isotopic compositions of photosynthetic pigments. Environ Microbiol 7: 1009−1016

Summons RE, Powell TG (1986) Chlorobiaceae in Palaeozoic seas - combined evidence from biological markers, isotopes and geology. Nature 319: 763−765

Tagami K, Uchida S (2008) Online stable carbon isotope ratio measurement in formic acid, acetic acid, methanol and ethanol in water by high performance liquid chromatography-isotope ratio mass spectrometry. Anal Chim Acta 614: 165−172